






## Original Research

# CCDC80 Induces Platinum Resistance in Ovarian Cancer Cells Through Epithelial-Mesenchymal Transition Pathway Activation

Li Xu<sup>1,†</sup>, Liulin Zhou<sup>2,†</sup>, Yixiao Wang<sup>1</sup>, Xiaohuan Jiang<sup>1</sup>, Yunlang Cai<sup>1,\*</sup><sup>1</sup>Department of Obstetrics and Gynecology, Zhongda Hospital, School of Medicine, Southeast University, 210009 Nanjing, Jiangsu, China<sup>2</sup>Department of Obstetrics and Gynecology, Taixing People's Hospital, 225400 Taizhou, Jiangsu, China\*Correspondence: [caiy12021@163.com](mailto:caiy12021@163.com) (Yunlang Cai)

†These authors contributed equally.

Academic Editors: Kenny Chitcholtan and Michael H. Dahan

Submitted: 25 April 2025 Revised: 13 June 2025 Accepted: 27 June 2025 Published: 22 August 2025

## Abstract

**Background:** The coiled-coil domain-containing protein 80 (CCDC80) has known roles in signal transduction and as a structural protein that stabilizes the extracellular matrix (ECM). *CCDC80* is also linked to drug resistance in cancers; however, the specific role of *CCDC80* in platinum resistance in ovarian cancer (OC) remains unclear. This study used a variety of gene analysis and complementary experimental approaches to examine the prognostic significance of *CCDC80* and the potential of this protein as a therapeutic target in OC. **Methods:** Differentially expressed genes (DEGs) were identified in the Gene Expression Omnibus (GEO) datasets (GSE15372, GSE51373, GSE114206) using the Limma package. The Kaplan-Meier analysis highlighted *CCDC80* as a key gene. Weighted gene co-expression network analysis (WGCNA) identified a *CCDC80*-related module as being enriched in cell chemotaxis and ECM remodeling pathways. Quantitative reverse transcription polymerase chain reaction, Western blotting, and immunohistochemistry were used to confirm *CCDC80* expression in platinum-resistant ovarian cancer (PROC) cell lines and clinical samples. Functional assays (cell count kit-8, colony formation, flow cytometry) were used to evaluate cisplatin sensitivity. Lastly, gene set enrichment analysis (GSEA), correlation analysis, and Western blotting were applied to investigate the mechanisms through which *CCDC80* affected the platinum resistance of OC cells. **Results:** The Limma package and Kaplan-Meier analysis identified *CCDC80* in the GEO datasets, and the WGCNA linked this protein to cell chemotaxis and ECM remodeling. The *CCDC80* mRNA and protein expression levels were shown to be significantly higher in PROC cell lines and ovarian cancer tissue samples. Functional assays indicated that *CCDC80* expression increases cisplatin resistance, while the GSEA and correlation analysis suggested that the epithelial-mesenchymal transition (EMT) pathway is a downstream target of *CCDC80*. Platinum resistance in OC cells was reduced by suppressing *CCDC80* expression and increased by stimulating EMT, confirming the role of the *CCDC80*-EMT axis in platinum resistance. **Conclusions:** This study shows that *CCDC80* expression is significantly elevated in platinum-resistant OC cells and that platinum resistance arises from CCDC-mediated activation of the EMT pathway. The *CCDC80*-EMT link provides a new understanding of the mechanisms leading to platinum resistance in OC and highlights *CCDC80* as a possible therapeutic target to prevent the development of chemotherapy resistance.

**Keywords:** *CCDC80*; platinum-resistant; ovarian cancer; epithelial-mesenchymal transition

## 1. Introduction

Ovarian cancer (OC) remains one of the most lethal gynecological malignancies worldwide. Approximately 90% of OC are epithelial ovarian carcinomas (EOCs) comprising distinct histological subtypes with specific molecular alterations, clinical behaviors, and treatment responses (the remaining 10% are non-epithelial tumors including germ cell tumors, sex cord-stromal tumors, and rare variants such as small cell carcinomas) [1–3]. The high mortality primarily stems from late-stage diagnosis and the development of chemotherapy resistance [1,2]. Platinum-based regimens are the mainstay treatment for EOCs, however, more than 70% of patients eventually develop resistance, leading to treatment failure [4,5]. Despite extensive research, the molecular mechanisms underlying EOC platinum resistance remain incompletely understood, currently limiting our ability to identify effective therapeutic targets.

Recent studies have implicated the tumor microenvironment as mediating the development of chemotherapy resistance via multiple mechanisms, including extracellular matrix (ECM) remodeling and cell-cell interactions [1,2]. Notably, the coiled-coil domain-containing protein 80 (CCDC80), a multifunctional protein involved in ECM stability and cell signaling [4,5], has emerged as a potential regulator of tumor progression and drug resistance in various cancers [6,7]. However, its specific role in OC platinum resistance remains unexplored, representing a significant knowledge gap in the field.

In this study, we investigated the function of *CCDC80* in platinum-resistant OC (PROC) using integrated bioinformatics and experimental approaches. We first established the expression pattern and prognostic value of *CCDC80* in ovarian cancer. Subsequent mechanistic studies revealed that *CCDC80* promotes platinum resistance by regulating



**Table 1. Patient characteristics.**

Characteristics	Categories	Cases (n)
Histological type	Serous	1232
	Endometrioid	62
Tumor stage	I	107
	II	72
	III	1079
	IV	189
Tumor grade	G1	56
	G2	325
	G3	1024
	G4	21

Note: Total sample size  $n = 1815$ . The sum of subgroups may not equal the total due to missing clinical information in some cases.

the epithelial-mesenchymal transition (EMT). These findings provide important new insights into OC drug resistance and identify *CCDC80* as a potential therapeutic target to prevent OC developing platinum resistance during chemotherapy regimes.

## 2. Materials and Methods

### 2.1 Data Acquisition and Preprocessing

Gene expression data from Gene Expression Omnibus (GEO) (GSE15372) were processed for background correction,  $\log_2$  transformation, and quantile normalization. Probes were mapped to gene symbols, and duplicates averaged. Using the Limma R package (v3.46.0, Bioconductor Core Team, Seattle, WA, USA), 907 differentially expressed genes (DEGs) were identified (538 downregulated, 369 upregulated) with  $\log_2$  fold change greater than 1.0 and an adjusted  $p$ -value less than 0.05. Cross-validation with datasets GSE51373 and GSE114206 confirmed consistent DEG expression trends.

### 2.2 Survival Analysis

Survival analysis was performed using the Kaplan-Meier Plotter online tool (<https://kmplot.com/analysis/>), which aggregates publicly available gene expression and clinical data from multiple ovarian cancer cohorts, including GSE14764, GSE15622, GSE18520, GSE19829, GSE23554, GSE26193, GSE26712, GSE27651, GSE30161, GSE3149, GSE51373, GSE63885, GSE65986, GSE9891, and The Cancer Genome Atlas (TCGA) (total  $n = 1815$  patients, Table 1).

### 2.3 Weighted Gene Co-expression Network Analysis (WGCNA) and Functional Enrichment Analysis

The WGCNA R package (v1.70, Bioconductor Core Team, Seattle, WA, USA) constructed a gene co-expression network with a soft threshold power of 10 for scale-free topology. Dynamic tree cut hierarchical clustering identified gene modules, and module-trait correlation analysis

pinpointed key modules linked to platinum resistance (640 genes). The Gene Ontology (GO) framework, which includes categories such as biological processes (BP), cellular components (CC), and molecular functions (MF), was utilized to functionally annotate these module genes through an integrated enrichment analysis in conjunction with the Kyoto Encyclopedia of Genes and Genomes (KEGG). Gene set enrichment analysis (GSEA) was conducted on The Cancer Genome Atlas-Ovarian Cancer (TCGA-OV) transcriptomic data to assess gene set enrichment from MSigDB (v2023.2, Broad Institute, Cambridge, MA, USA). The clusterProfiler R package (v4.10.0, Bioconductor Core Team, Seattle, WA, USA) calculated the normalized enrichment score (NES), identifying significant pathways with a false discovery rate (FDR)  $< 0.05$ .

### 2.4 Immunohistochemistry (IHC) and Pathological Examination

Paraffin tissue blocks from Zhongda Hospital, Southeast University, were sectioned to 3  $\mu\text{m}$ . To retrieve antigens, samples were treated in a Tris-EDTA buffer (Solarbio, Cat#1033, Beijing, China) at pH 8 and 98  $^{\circ}\text{C}$  for 40 min, and endogenous peroxidase was neutralized with 3% hydrogen peroxide for 10 min. The tissue sections were incubated overnight at 4  $^{\circ}\text{C}$  with a rabbit anti-human *CCDC80* antibody (Absin, Cat#abs127221, Shanghai, China; dilution 1:200). Subsequently, they were treated with an HRP-conjugated secondary antibody (Aifang Biotechnology, Cat#AFIHC004, Beijing, China; dilution 1:1) at room temperature for 50 min. Following this, the sections were counterstained with hematoxylin, fixed, dehydrated, and subjected to microscopic imaging post-color development.

### 2.5 Cell-based Experiments

#### 2.5.1 Experimental Design and Statistical Rigor

All experiments were performed with randomization and blinding. Each experimental condition was independently repeated  $\geq 3$  times (biological replicates) using freshly prepared cells. Group allocation and sample processing order were randomized and performed by researchers not involved in data analysis.

#### 2.5.2 Cell Culture and Transfection

The SKOV3 cell line was kindly provided by Dr. Hui Xu from the Department of Immunology, Southeast University School of Medicine. The SKOV3/DDP human cell line was purchased from Shanghai Jinyuan Biotechnology Co., Ltd. All cell lines were authenticated by STR profiling matching with ATCC databases and confirmed to be mycoplasma-free by PCR testing. Cells were cultured in McCoy's 5A medium (KeyGen Biotech, Cat#KGL1701-500, Nanjing, Jiangsu, China) with added supplements, including 10% fetal bovine serum (KeyGen Biotech, Cat#11011-9611, Nanjing, Jiangsu, China), 100  $\mu\text{g}/\text{mL}$  penicillin, and 100  $\mu\text{g}/\text{mL}$  streptomycin (Beyotime,

Cat#C0222, Shanghai, China). *CCDC80* knockdown (sh-*CCDC80*) and control (empty vector negative control, sh-NC) lentiviruses were produced by GenePharma (Shanghai, China). Transfections were performed following the manufacturer's instructions, with medium replacement after 24 h. Stable transfectants were selected using 2 µg/mL puromycin (Biotech, Cat#ST551, Shanghai, China) for 2–3 generations.

### 2.5.3 Quantitative Reverse Transcription Polymerase Chain Reaction (qRT-PCR)

RNA extraction from cell samples was conducted utilizing the TRIzol reagent (Vazyme Biotech, Cat#R401-01, Nanjing, Jiangsu, China). Subsequent reverse transcription was performed employing the HiScript II Reverse Transcription Kit (Vazyme Biotech, Cat#R323-01, Nanjing, Jiangsu, China). qPCR was executed using SYBR Green dye (Vazyme Biotech, Cat#Q712-02, Nanjing, Jiangsu, China), with each sample analyzed in triplicate. Gene expression was quantified utilizing the  $2^{-\Delta\Delta CT}$  method, employing glyceraldehyde-3-phosphate dehydrogenase (*GAPDH*) as the reference gene. The primer sequences were as follows:

*CCDC80* (forward): 5'-GACCCCGTTTCACTATGCTGT-3'

*CCDC80* (reverse): 5'-GGCGAGCTAGTCTCAACACG-3'

*GAPDH* (forward): 5'-ACAGTCAGCCGCATCTTCTT-3'

*GAPDH* (reverse): 5'-GACAAGCTTCCCGTTCTCAG-3'

### 2.5.4 Western Blotting Assay

RIPA buffer (Beyotime, Cat #P0013, Shanghai, China) along with protease inhibitors (Servicebio, G2008, Wuhan, Hubei, China) was used to lyse the cells. Protein samples were resolved via 4%–20% sodium dodecyl sulfate–polyacrylamide gel electrophoresis (SDS-PAGE) (ACE, Cat #F11420Gel, Changzhou, Jiangsu, China) and subsequently transferred onto polyvinylidene fluoride membranes (Millipore, Cat#ISEQ00010, Burlington, MA, USA). The membranes were blocked with 5% skim milk at ambient temperature and subsequently incubated overnight at 4 °C containing primary antibody specific for *CCDC80* (Thermo Fisher, Cat #PA5-45821, Waltham, MA, USA; diluted 1:500), E-cadherin (Proteintech, Cat #20874-1-AP, Wuhan, Hubei, China; diluted 1:2000), VIM (Proteintech, Cat #60330-1-Ig, Wuhan, Hubei, China; diluted 1:2000), or  $\alpha$ -SMA (Proteintech, Cat #14395-1-AP, Wuhan, Hubei, China; diluted 1:2000). After washing three times with Tris-Buffered Saline with Tween 20 (TBST; Beyotime, Cat #ST825, Shanghai, China), the membranes were incubated for 1 h at room temperature containing HRP-conjugated rabbit secondary antibody (Proteintech, Cat #SA00001-2, Wuhan, Hubei, China; diluted 1:5000). An HRP-

conjugated *GAPDH* antibody (Abways, Cat #AB0037, Shanghai, China; diluted 1:5000) served as the internal control. Signal detection was performed using a hypersensitive chemiluminescence kit (Beyotime, Cat#P0013, Shanghai, China), with image capture executed via a Tanon 5200 (Tianneng Technology Co., Ltd., Shanghai, China) automatic chemiluminescence imaging system, and signal quantification conducted using Image J software (v1.54f; National Institute of Health, Bethesda, MD, USA).

### 2.5.5 Cell Count Assay

Cell viability was evaluated utilizing the Cell Counting Kit-8 (CCK-8) assay (Biosharp, Cat#K101837133EF5E, Hefei, Anhui, China). Cells in logarithmic growth phase were seeded into 96-well plates (WHB, Cat #WHB-96, Shanghai, China) at a density of  $1 \times 10^4$  cells per well, with the peripheral wells filled with phosphate buffered saline (PBS; iLab, Cat#AC08L011, Shanghai, China) to mitigate edge effects. Following cell attachment, the culture medium was replaced with cisplatin solutions at varying concentrations (0, 0.3, 1, 3, 10, 30, and 100 µg/mL). Each concentration was tested in triplicate, and the experiments were independently conducted three times. After incubation periods of 24 and 48 h, 10 µL of CCK-8 solution was added to each well, and the plates were incubated at 37 °C with 5% CO<sub>2</sub> for an additional 3 h. Absorbance at 450 nm was measured using a microplate reader (BIOTEK, Agilent Technologies, Winooski, VT, USA). Dose-response curves were fitted using a 4-parameter logistic model (v10.0, GraphPad Software, San Diego, CA, USA) with variable slope. Half maximal inhibitory concentration (IC<sub>50</sub>) values and 95% confidence intervals (Profile Likelihood) were derived from triplicate experiments. Group comparisons were performed via Extra sum-of-squares F test (curve fits) or Mann-Whitney U test (non-normal distributions).

### 2.5.6 Apoptosis Assay

Cell apoptosis was assessed using the Annexin V–Fluorescein Isothiocyanate (V-FITC)/propidium iodide (PI) Apoptosis Detection Kit (Elabscience, Cat #E-CK-A211, Wuhan, Hubei, China) and quantified by flow cytometry. Single-cell suspensions were generated via trypsinization without ethylenediaminetetraacetic acid (Beyotime, Cat#C0205, Shanghai, China) and subsequently washed with ice-cold PBS. The cells were incubated with recombinant human Annexin V-FITC for 5 min at room temperature in the dark, followed by a 30-minute incubation with PI at 4 °C in the dark. Apoptotic cells were identified using a BD FACSCelesta flow cytometer (BD Biosciences, Cat #657231, Becton Drive, Franklin Lakes, NJ, USA), and the resulting data were analyzed with FlowJo software (v10.5.0, National Institutes of Health, Bethesda, MD, USA).

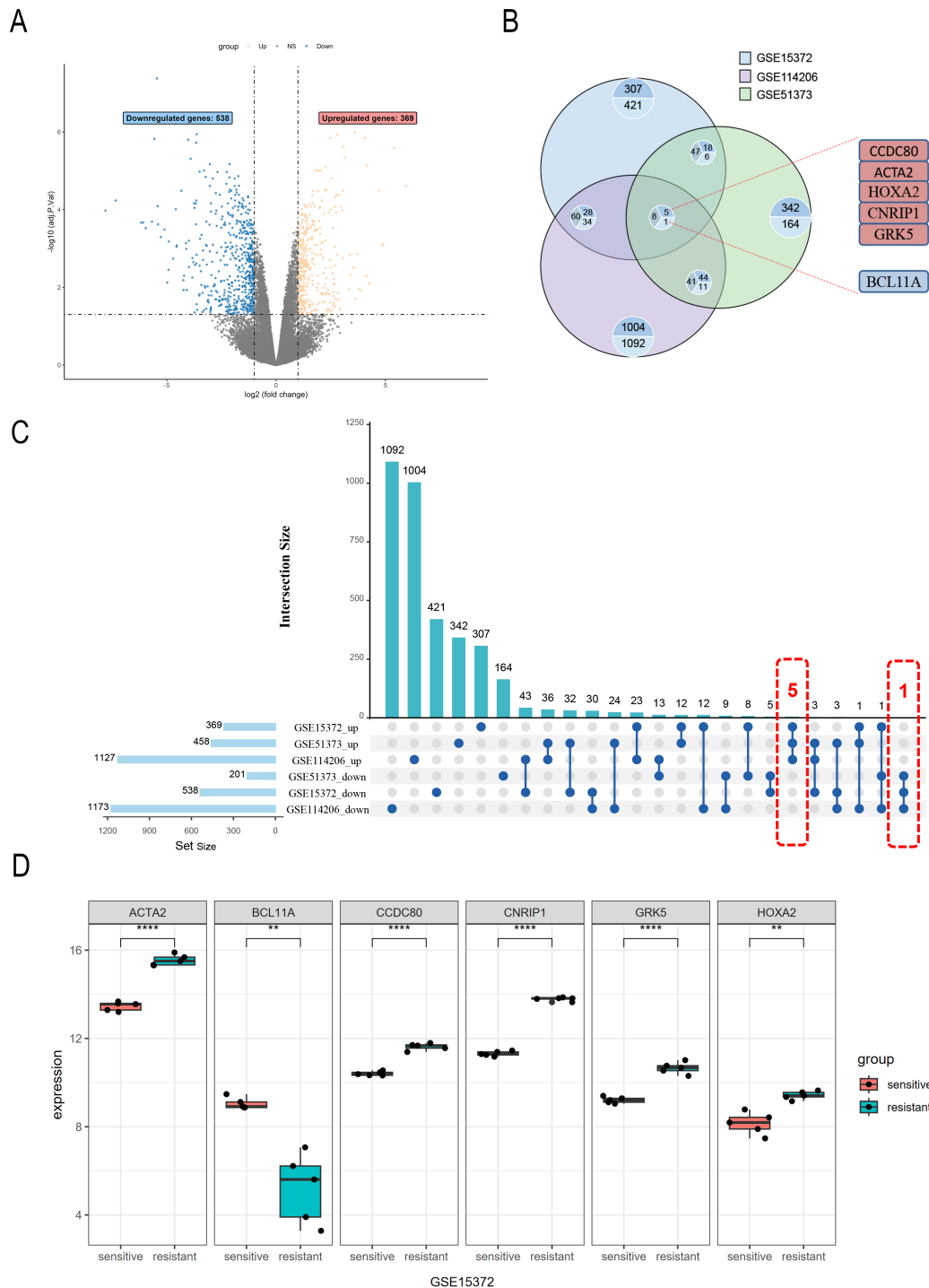


**Fig. 1. Differential gene expression analysis in PROC datasets.** (A) The GSE15372 dataset includes six cisplatin-resistant and six cisplatin-sensitive ovarian cancer cell samples; 369 upregulated genes and 538 downregulated genes are identified. Genes with non-significant changes in expression are shown in gray. (B) Intersection analysis of upregulated and downregulated genes from the GSE15372, GSE114206, and GSE51373 datasets. (C) The Upset plot illustrates the overlap of upregulated and downregulated genes across the three datasets, and the number of genes in each set. (D) Expression levels of differentially expressed genes (*ACTA2*, *CCDC80*, *CNRIP1*, *GRK5*, *HOXA2*, and *BCL11A*) in the GSE15372 dataset. *ACTA2*, *CCDC80*, *CNRIP1*, and *GRK5* (\*\*\*\*  $p < 0.0001$ ); *HOXA2* and *BCL11A* (\*\*  $p < 0.01$ ). PROC, platinum-resistant ovarian cancer; GSE, Gene Expression Omnibus Series Entry; *ACTA2*, actin alpha 2, smooth muscle; *CCDC80*, coiled-coil domain-containing protein 80; *CNRIP1*, cannabinoid receptor interacting protein 1; *GRK5*, g protein-coupled receptor kinase 5; *HOXA2*, homeobox A2; *BCL11A*, B-Cell lymphoma/leukemia 11a.



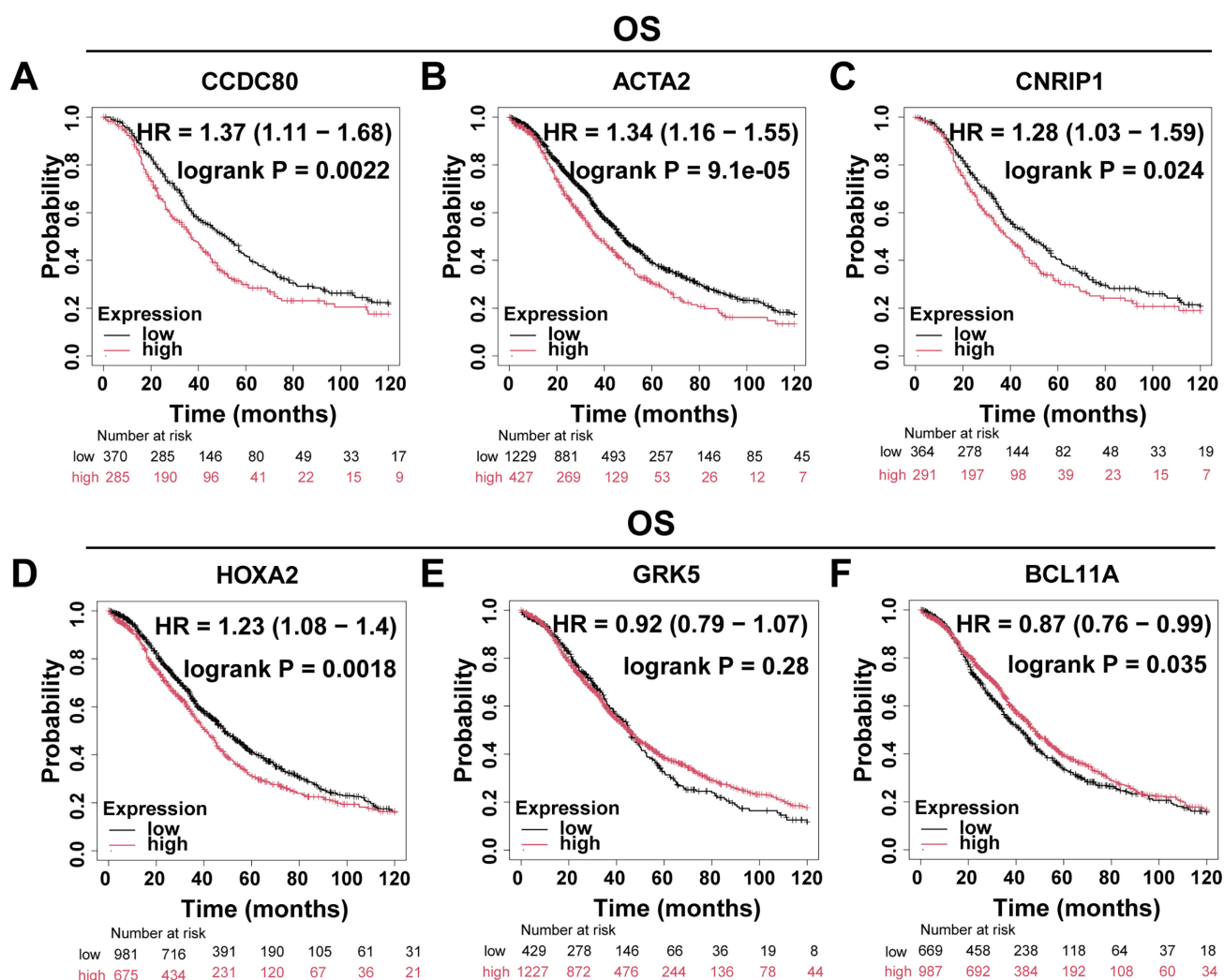


**Fig. 2. Differential gene OS analysis.** Patients with OC were divided into two groups based on gene expression levels, and Kaplan-Meier curves were used to compare the overall survival rates between these two groups. (A) *CCDC80* (n = 655). (B) *ACTA2* (n = 1656). (C) *CNRIP1* (n = 655). (D) *HOXA2* (n = 1656). (E) *GRK5* (n = 1656). (F) *BCL11A* (n = 1656). OS, overall survival; HR, hazard ratio.

### 2.5.7 Colony-formation Assay

Exponential phase cells were exposed for 24 h to 5  $\mu$ g/mL cisplatin (MACKLIN, Cat # D807330, Shanghai, China), then seeded into 6-well plates (WHB, Cat #WHB-6, Shanghai, China) at a density of 1000 cells per well. The cells were subsequently cultured at 37 °C in an atmosphere containing 5% CO<sub>2</sub> until macrocolonies (consisting of more than 50 cells per colony) had formed. The colonies were then fixed for 30 min using 100% methanol (Biosharp, Cat #BL539A, Hefei, Anhui, China) and stained with a 0.1% crystal violet solution (Beyotime, Cat # C0121, Shanghai, China) for 30 min.

## 3. Results

### 3.1 Identification of DEGs

To explore the DEGs associated with PROC, we procured raw gene expression data from the GEO database (accession number: GSE15372). Following data prepro-

cessing and normalization of the expression matrices across all datasets (**Supplementary Fig. 1**), we identified a total of 907 DEGs, comprised of 538 downregulated and 369 upregulated genes (Fig. 1A). Subsequent cross-validation using datasets GSE51373 and GSE114206 (Fig. 1B,C) revealed six co-expressed genes exhibiting consistent expression patterns (**Supplementary Table 1**). These include the upregulated genes *CCDC80*, *ACTA2*, *HOXA2*, *CNRIP1*, and *GRK5*, and the downregulated gene *BCL11A* (Fig. 1D).

### 3.2 Prognostic Implications of DEGs

The Kaplan-Meier Plotter platform (<https://kmplot.com/analysis/>) was utilized to evaluate the Overall Survival (OS) and progression-free survival (PFS) of DEGs. The findings indicated that the expression levels of *CCDC80*, *ACTA2*, *HOXA2*, and *BCL11A* were significantly correlated with OS (Fig. 2A–F) and PFS (Fig. 3A–F) in patients with OC. Notably, *CCDC80* demonstrated the highest hazard ra-

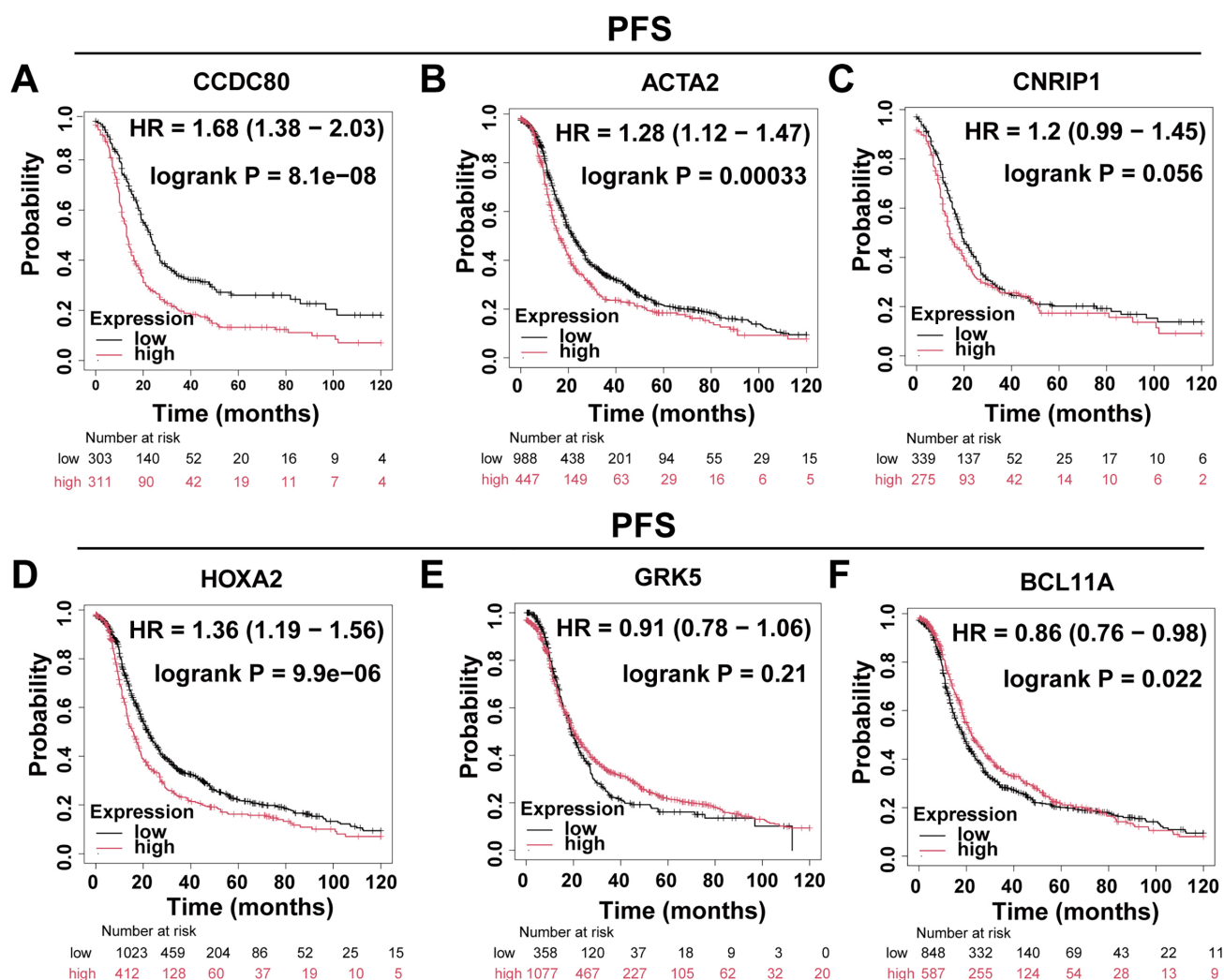


**Fig. 3. Differential gene PFS analysis.** Patients with ovarian cancer were divided into two groups based on gene expression levels, and Kaplan-Meier curves were used to compare progression-free survival between these groups. (A) *CCDC80* (n = 614). (B) *ACTA2* (n = 1435). (C) *CNRIP1* (n = 614). (D) *HOXA2* (n = 1435). (E) *GRK5* (n = 1435). (F) *BCL11A* (n = 1435). PFS, progression-free survival.

tio (HR) for both OS and PFS, identifying it as the principal gene warranting further investigation.

### 3.3 Identification of Key Gene Modules

WGCNA was conducted to establish a co-expression network of DEGs. To maintain analytical precision, a soft threshold power of 10 was applied to delineate gene relationships within the dataset (Fig. 4A). Hierarchical clustering of the entire gene set unveiled several gene modules exhibiting significant co-expression patterns (Fig. 4B). Notably, the METurquoise module demonstrated a robust correlation with platinum resistance and was consequently selected for further investigation due to its statistical significance (Fig. 4C).

### 3.4 GO and KEGG Enrichment Analysis

To elucidate the biological functions of key module genes, we conducted GO and KEGG enrichment analy-

ses. The GO analysis revealed that these genes are predominantly involved in cell chemotaxis and ECM organization (Fig. 5A). Chord diagrams further demonstrated that the majority of genes within these pathways were down-regulated, indicating a suppression of related pathways in PROC (Fig. 5B–D). The KEGG pathway analysis indicated that, alongside the suppression of cytokine-cytokine receptor interactions and ECM-receptor interactions, the PI3K-AKT signaling pathway was also significantly downregulated (Fig. 5E,F). These findings suggest that the expression of key genes facilitates ECM remodeling and affects cell chemotaxis, potentially closely linking them to chemotherapy resistance in OC.

### 3.5 Investigation of *CCDC80* Expression in PROC

We analyzed the expression pattern of *CCDC80* in PROC tissues by comparing its expression levels in two PROC tissue samples with those in four platinum-sensitive

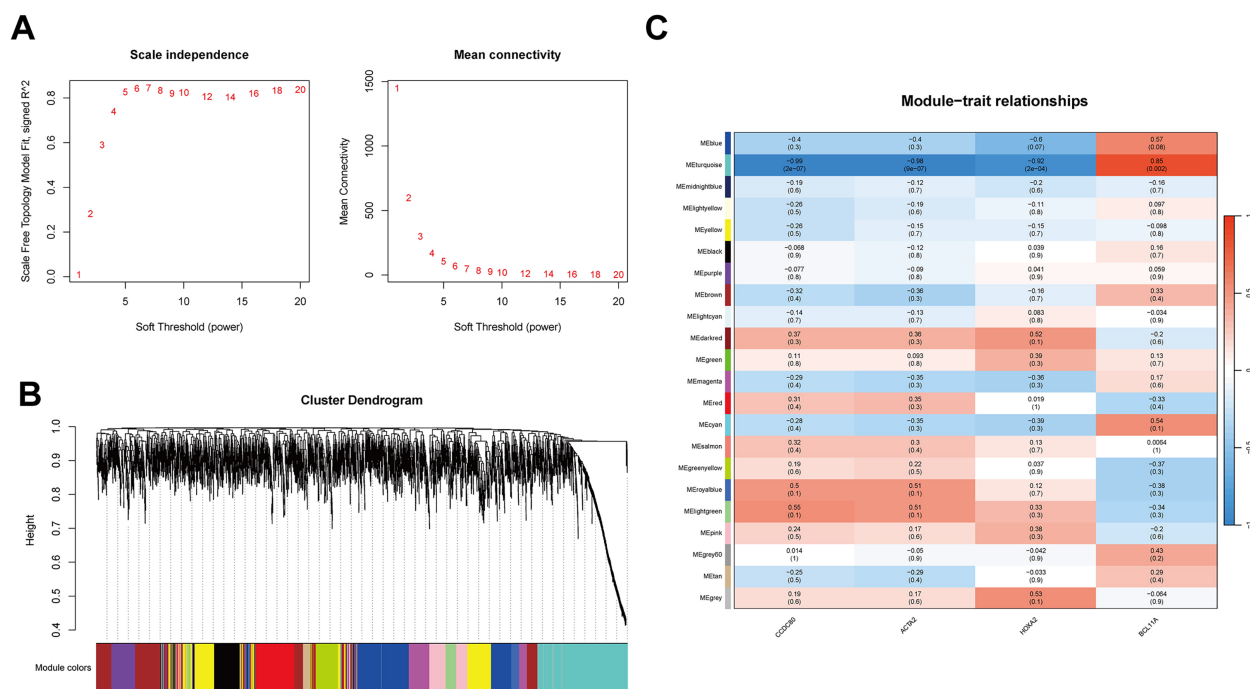


**Fig. 4. WGCNA and biological function analysis.** (A) Selection of the soft threshold (power = 10) for WGCNA using scale independence and average connectivity. (B) Gene clustering dendrogram of the 21 modules identified by WGCNA. Branches of the dendrogram represent genes, with those showing similar expression clustered within the same module (color-coded). (C) Heatmap showing the correlation between WGCNA network modules and *CCDC80*, *ACTA2*, *HOXA2*, and *BCL11A*. WGCNA, weighted gene co-expression network analysis.

OC tissue samples (**Supplementary Table 2**). The findings revealed a significant elevation of *CCDC80* expression in PROC tissues, predominantly localized within the cytoplasm and cell membrane (Fig. 6A). Subsequent validation using cisplatin-resistant SKOV3 cells (SKOV3/DDP) demonstrated a marked upregulation of *CCDC80* expression at the level of both mRNA and protein (Fig. 6B,C).

### 3.6 *CCDC80* Knockdown Enhances OC Cell Sensitivity to Cisplatin

To assess the role of *CCDC80* in modulating the sensitivity of OC cells to platinum-based chemotherapy, SKOV3/DDP cells were transfected with *CCDC80* shRNA (sh-*CCDC80*). Western blot analysis confirmed that this treatment induced a marked reduction in *CCDC80* protein levels compared to cells transfected with the empty vector negative control (sh-NC) (Fig. 7A). The half-maximal IC<sub>50</sub> of cisplatin was measured for both sh-*CCDC80* and sh-NC cells, revealing significantly lower IC<sub>50</sub> values for the sh-*CCDC80* cells at 24 h (10.27  $\mu$ g/mL, 95% CI: 9.610–10.96) and 48 h (3.11  $\mu$ g/mL, 95% CI: 2.554–3.768) compared to sh-NC cells (38.95  $\mu$ g/mL, 95% CI: 31.56–48.90 at 24 h; 8.43  $\mu$ g/mL, 95% CI: 6.794–10.48 at 48 h) (Fig. 7B). Flow cytometry analysis indicated that knock down of *CCDC80* expression induced a significant increase in cisplatin-induced SKOV3/DDP cell apoptosis (Fig. 7C). Furthermore, colony formation assays indicated that sup-

pression of *CCDC80* expression substantially increased the sensitivity of SKOV3/DDP cells to cisplatin (Fig. 7D). Overall, the results indicate that reduced *CCDC80* expression lowers the resistance of SKOV3/DDP cells to cisplatin.

### 3.7 *CCDC80* Modulates EMT in SKOV3/DDP Cells

The previous results indicated that *CCDC80* plays a role in ECM formation. GSEA utilizing TCGA-OV data demonstrated a negative correlation between the expression of *CDH1* (which encodes E-cadherin) and *CCDC80* (Fig. 8A). Furthermore, analysis of the GSE15372 dataset revealed a strong positive correlation between *CCDC80* and *ACTA2* (which encodes  $\alpha$ -SMA) (Fig. 8B). Together, these observations suggest a significant association between the upregulation of *CCDC80* and EMT. Silencing of *CCDC80* in SKOV3/DDP cells led to a decrease in  $\alpha$ -SMA and VIM protein expression and an increase in E-cadherin protein expression (Fig. 8C), thereby confirming the regulatory role of *CCDC80* in the EMT phenotype of OC cells. Upregulation of EMT partially restored cisplatin resistance in sh-*CCDC80*-SKOV3/DDP cells, with IC<sub>50</sub> values of 18.14  $\mu$ g/mL and 5.994  $\mu$ g/mL at 24 and 48 h, respectively (Fig. 8D). Colony formation assays provided additional evidence that the upregulation of EMT increased cisplatin resistance in sh-*CCDC80*-SKOV3/DDP cells (Fig. 8E). Flow cytometry analysis indicated that treatment with TGF- $\beta$ 1 significantly decreased cell apoptosis (Fig. 8F). These find-

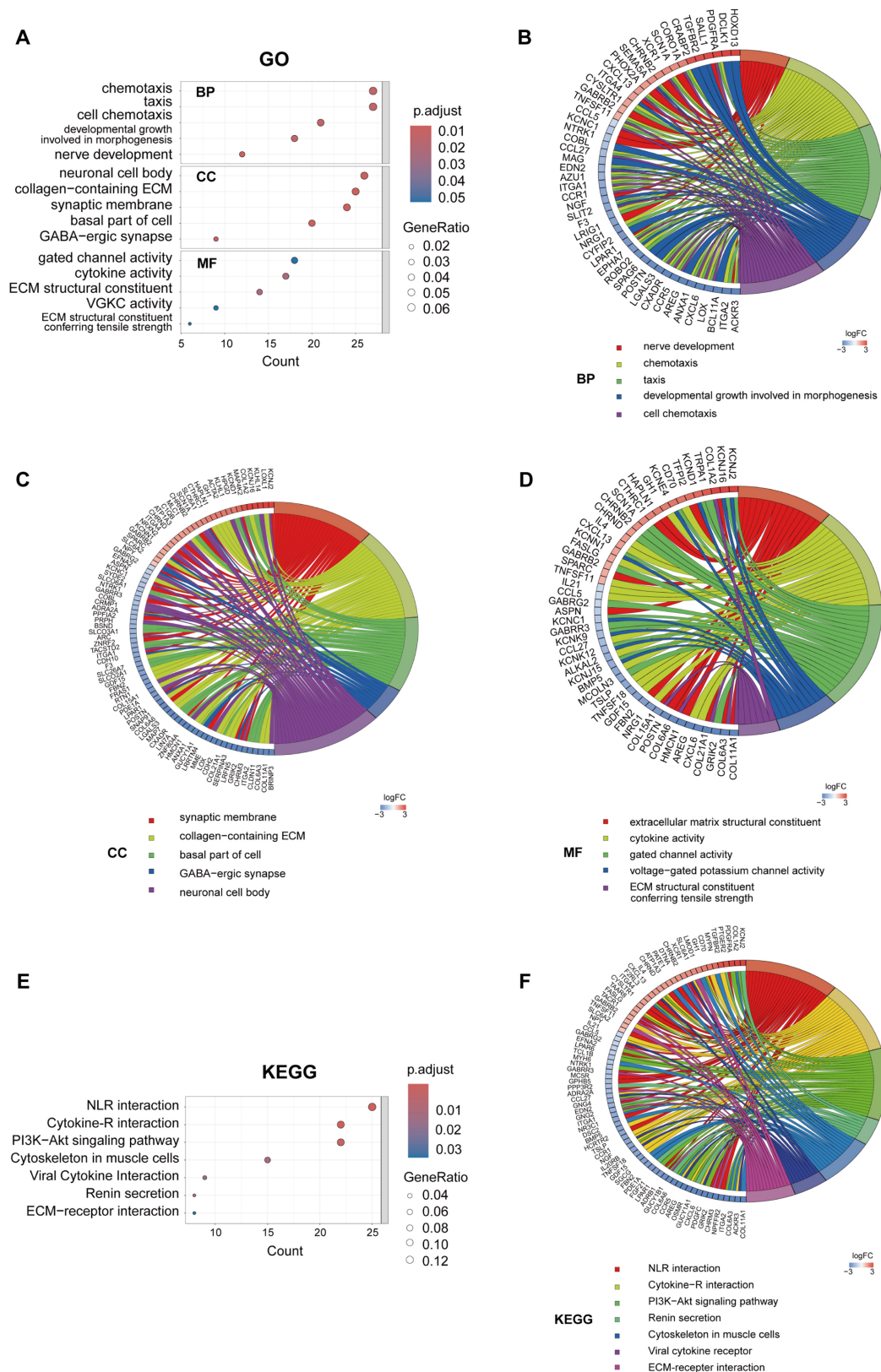


**Fig. 5. GO and KEGG analysis of the MEturquoise module.** (A) GO enrichment analysis of: biological processes (BP), cellular components (CC), and molecular functions (MF). GO enrichment chord diagrams displaying biological processes (B), cellular components (C) and molecular functions (D). (E) KEGG enrichment analysis. (F) KEGG enrichment chord diagram. GO, Gene Ontology; KEGG, Kyoto Encyclopedia of Genes and Genomes; ECM, extracellular matrix; NLR, neuroactive ligand-receptor interaction.



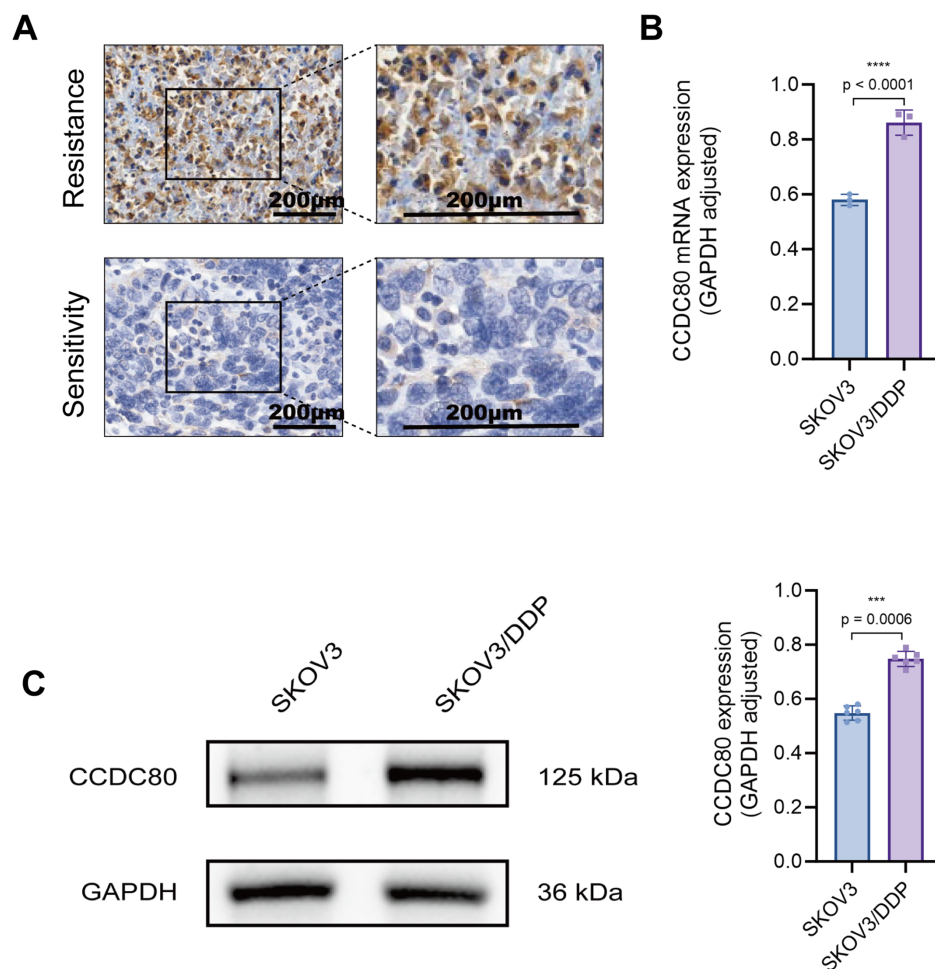


**Fig. 6. Validation of *CCDC80* expression in clinical samples and cell lines.** (A) Immunohistochemical detection of *CCDC80* in platinum-resistant and platinum-sensitive ovarian cancer tissues. (B) RT-PCR analysis of *CCDC80* mRNA in platinum-sensitive and resistant ovarian cancer cell lines. (C) Western blot of *CCDC80* protein in platinum-sensitive and resistant ovarian cancer cell lines. RT-PCR, quantitative reverse transcription polymerase chain reaction; *GAPDH*, glyceraldehyde-3-phosphate dehydrogenase; SKOV3, human ovarian adenocarcinoma cell line; DDP, cisplatin (cis-diammine-dichloroplatinum); \*\*\*  $p < 0.001$ ; \*\*\*\*  $p < 0.0001$ . Scale bar = 200 µm

ings establish that *CCDC80* enhances the resistance of SKOV3/DDP OC cells to platinum by upregulating EMT.

#### 4. Discussion

This study is the first focused investigation into the critical role of *CCDC80* in mediating platinum resistance in ovarian cancer cells. The findings reveal a significant up-regulation of *CCDC80* in patient-derived platinum-resistant ovarian cancer, and indicate that in SKOV3/DDP cells enhanced *CCDC80* expression increases platinum resistance by stimulating the EMT pathway. These findings provide insights into the molecular mechanisms underlying platinum resistance in ovarian cancer, and identify *CCDC80* as a new therapeutic target that offers the potential to avoid OC developing platinum resistance during patient chemotherapy.

*CCDC80* was previously classified as a tumor suppressor gene [8–11]. However, recent research has elucidated its involvement in promoting treatment resistance and immune tolerance in certain malignancies, with some studies suggesting its potential as a prognostic biomarker for adverse outcomes [6,7,12]. This study is the first to demonstrate that *CCDC80* is significantly upregulated in PROC, strongly correlating with poor patient prognosis.

The increased stemness of tumor cells is a critical factor contributing to chemotherapy resistance in ovarian cancer [13–15]. EMT is pivotal in modulating tumor stemness [16,17]. Key transcription factors, including Snail and zinc finger e-box binding homeobox 1 (ZEB1), together with signaling pathways such as Wnt/ $\beta$ -catenin, serve as primary instigators of EMT [18–21]. These elements initiate EMT by both downregulating epithelial markers and upregulat-

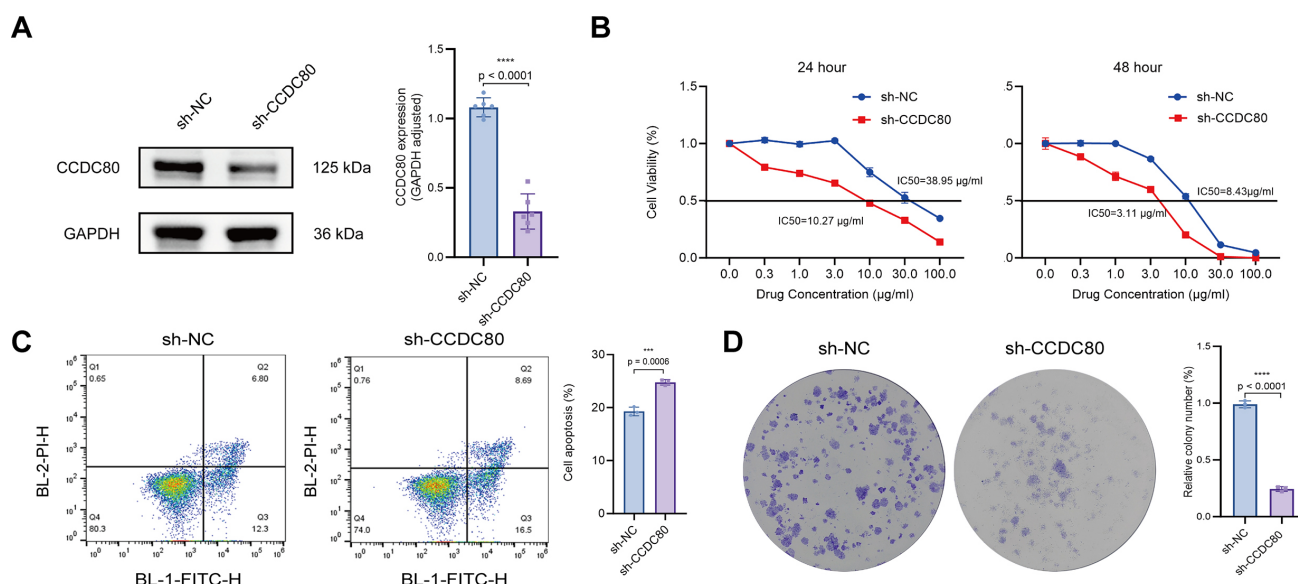


**Fig. 7. *CCDC80* knockdown reverses cisplatin resistance in SKOV3/DDP cells.** (A) Western blot confirms lentivirus-mediated knockdown of *CCDC80* expression. (B) IC<sub>50</sub> of cisplatin for cells before and after knock-down of *CCDC80* expression. (C) Flow cytometric quantification of cell apoptosis following treatment for 24 h with 38  $\mu\text{g/ml}$  cisplatin. Results are shown for cells transfected to knock down *CCDC80* expression, and untransfected control cells. (D) Colony-forming ability of untransfected cells and cells transfected to knock down *CCDC80* expression, when exposed to 38  $\mu\text{g/ml}$  cisplatin for 24 h. sh-NC, empty vector negative control; IC<sub>50</sub>, inhibitory concentration; BL-2-PI-H, blue laser detector 2-propidium iodide, height signal detection channel; BL-1-FITC-H, blue laser detector 1-fluorescein isothiocyanate, height signal detection channel. \*\*\*  $p < 0.001$ ; \*\*\*\*  $p < 0.0001$ .

ing mesenchymal markers. Concurrently, the EMT process enhances the activity of the above mentioned transcription factors and signaling pathways, to establish a positive feedback loop. This dynamic interaction ultimately results in the upregulation of genes associated with stemness, such as Nanog and Oct4, which provide tumor cells with stem cell-like properties [22] and an accompanying resistance to chemotherapeutic drugs, including platinum-based drugs [23]. This resistance is facilitated through mechanisms such as enhanced DNA repair, inhibition of apoptosis, increased drug efflux, and metabolic reprogramming [17]. *CCDC80* is regarded as a potential prognostic marker of stemness [6,12]. Our findings indicate that in SKOV3/DDP cells, *CCDC80* upregulation is correlated with decreased expression of E-cadherin and increased expression of  $\alpha$ -SMA and VIM. This suggested that *CCDC80* facilitates tumor cell drug resistance by promoting the EMT phenotype. Further experiments showed that stimulation of EMT partially reinstates the resistance of sh-*CCDC80*-SKOV3/DDP cells to cisplatin, underscoring the pivotal role of the *CCDC80*-EMT axis in mediating resistance to platinum-based drugs.

Functional enrichment analyses demonstrate that *CCDC80* upregulation significantly enhances cellular chemotaxis. Mechanistically, this augmented chemotactic activity facilitates the formation of a dense stromal barrier that substantially impedes drug penetration—a phenomenon that aligns precisely with *CCDC80*'s established role in ECM organization [22,24]. Moreover, we also

showed that *CCDC80* upregulation mediates downregulation of the PI3K-AKT signaling pathway, which promotes chemotherapy resistance by enhancing cell survival, inhibiting apoptosis, and modulating the tumor microenvironment [25–27]. One possible explanation for the *CCDC80*-induced downregulation of PI3-AKT activity is that, when exposed to platinum, tumors may adapt by relying on alternative survival mechanisms, such as those provided by the MAPK or JAK-STAT pathways [28–30]. The redundancy in survival pathways underscores the complexity of resistance mechanisms and highlights the need to explore their interactions. Furthermore, reduced PI3K-AKT activity could provide a metabolic advantage to platinum-resistant cells. Given that PI3K-AKT regulates glucose metabolism and anabolic processes, its suppression might drive resistant cells to adopt a more energy-efficient metabolic phenotype, such as increased reliance on oxidative phosphorylation, enabling them to better survive chemotherapy-induced stress [31–34].

The emergence of drug resistance is a substantial clinical obstacle to the use of platinum-based chemotherapeutic agents, which are the cornerstone of OC treatment. Reinforcing the clinical importance of platinum resistance, BRCA1/2 germline mutations are the strongest known genetic risk factor for epithelial OC and occur in 6–15% of patients — these mutations confer enhanced platinum sensitivity and result in superior survival outcomes, despite typically later-stage and higher-grade diagnosis [34,35].

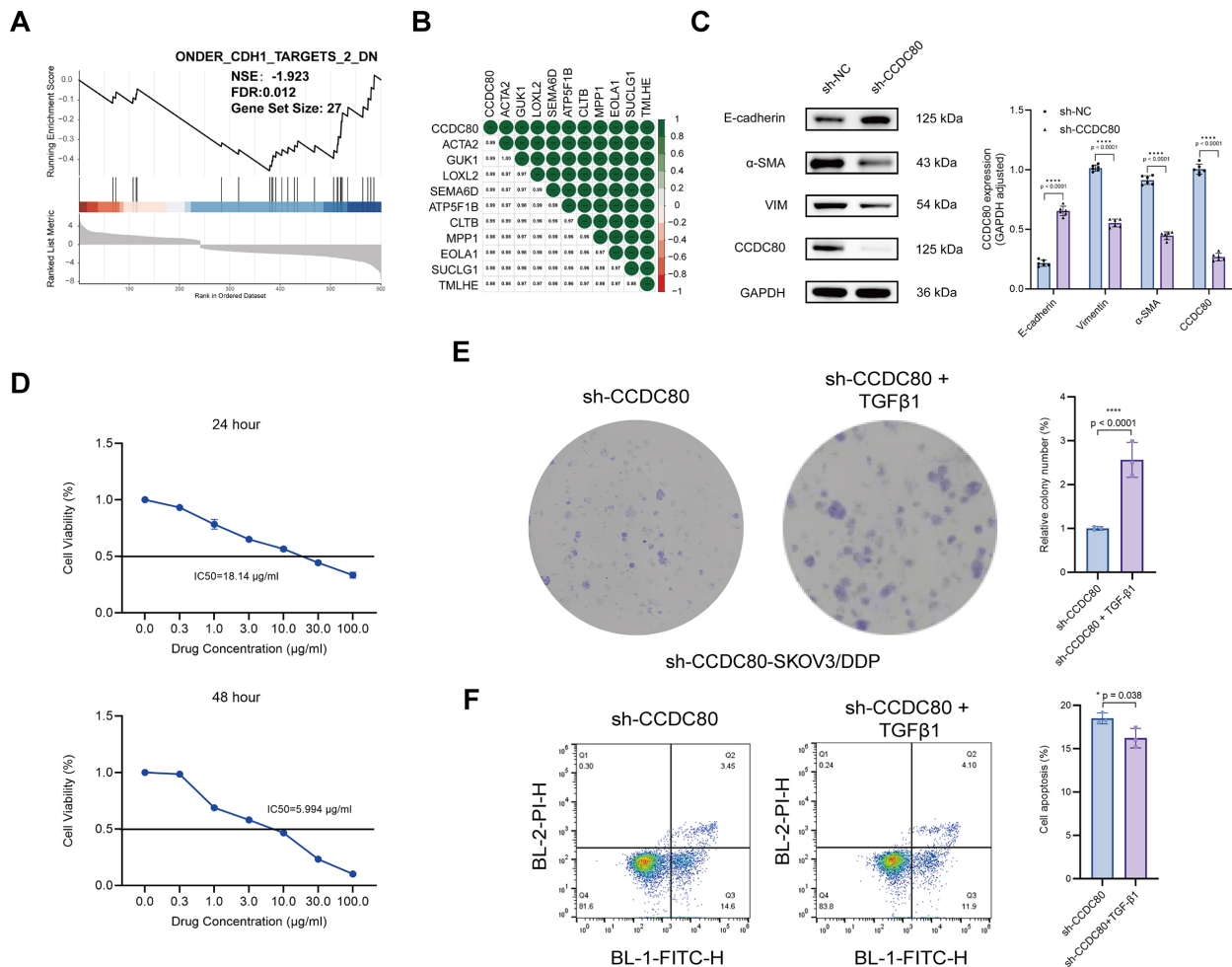


**Fig. 8.** *CCDC80* mediates platinum resistance in SKOV3/DDP cells by upregulating EMT. (A) GSEA analysis. (B) *CCDC80* gene correlation analysis. (C) *CCDC80* knockdown reduces EMT phenotype. (D) Cisplatin IC<sub>50</sub> in sh-*CCDC80*-SKOV3/DDP cells pre- and post-EMT induction. (E) Colony-forming ability of sh-*CCDC80*-SKOV3/DDP cells treated with 18 μg/mL cisplatin for 24 h, before and after EMT induction. (F) Flow cytometric quantification of apoptosis in EMT-induced and control sh-*CCDC80*-SKOV3/DDP cells following treatment for 24 h with 18 μg/mL cisplatin. EMT, epithelial-mesenchymal transition; \*  $p < 0.05$ ; \*\*\*\*  $p < 0.0001$ .

The development of specific and potent inhibitors targeting *CCDC80*, alongside the refinement of delivery systems, such as nanoparticle-based platforms, may offer a novel therapeutic approach to counteract drug resistance [7,36,37]. Moreover, *CCDC80* expression levels could potentially serve as biomarkers for predicting the efficacy of platinum-based chemotherapy, thereby establishing a basis for personalized treatment strategies [6,12,38].

While this study significantly advances our understanding of the role of *CCDC80* in mediating platinum resistance in OC, several limitations remain, and warrant further investigation. First, the precise molecular mechanisms by which *CCDC80* regulates EMT, particularly its downstream signaling and interactions with TGF- $\beta$ /Wnt pathways, require further elucidation. Second, the clinical validation was limited by a small sample size ( $n = 6$ ) without covariate matching, despite pathological confirmation (tumor content >70%) and absence of systematic differ-

ences in key clinical variables (e.g., staging, histology). Future prognostic model development will employ larger cohorts with proper matching. Finally, while our cellular-level findings demonstrate the role of *CCDC80* in platinum resistance in SKOV3/DDP cells, animal studies are needed to validate these observations, which will be incorporated in subsequent investigations of *CCDC80*-regulated EMT mechanisms. Other directions to prioritize in future research include: (1) Examine the efficacy of combined treatments that include *CCDC80* silencing, PARP inhibition and immune checkpoint blockade, particularly in homologous recombination deficient (HRD) tumors. This approach may enhance tumor immunogenicity and overcome resistance through modulation of neoantigen load, STING-interferon pathway, and PARP inhibitor-induced immunomodulation (e.g., GSK3 inactivation/PD-L1 upregulation) [26,34–38]; (2) Examine the role of *CCDC80* in metastasis, angiogenesis, and metabolic reprogramming, to further illumi-

nate its contributions to tumor biology; (3) Integrate high-throughput proteomics with functional validation studies to identify additional *CCDC80*-regulated protein interaction networks underlying drug resistance. This could provide a molecular basis for the development of additional combination targeting strategies.

## 5. Conclusions

This study is the first to demonstrate that (i) *CCDC80* expression is increased in platinum-resistant patient OC, correlating with unfavorable patient prognosis, and (ii) in SKOV3/DDP OC cells, *CCDC80* promotes platinum resistance by activating the EMT pathway. These findings implicate *CCDC80* as a potential therapeutic target, and may ultimately lead to the development of new treatments to improve the survival rates of OC patients.

## Availability of Data and Materials

The datasets used and analysed during the current study are available from the corresponding author on reasonable request.

## Author Contributions

LX, LZ and YC designed the research protocol and established the analytical methodology. LX performed the molecular experiments. YW conducted the immunohistochemical assays. LX led the bioinformatics analysis. LZ and XJ assisting in data visualization. YC, the Principal Investigator, secured funding and resources and oversaw the research with critical review. All authors contributed to editorial changes in the manuscript. All authors read and approved the final manuscript. All authors have participated sufficiently in the work and agreed to be accountable for all aspects of the work.

## Ethics Approval and Consent to Participate

The study was carried out in accordance with the guidelines of the Declaration of Helsinki, and the protocol was approved by the Ethics Committee of Zhongda Hospital Affiliated to Southeast University, Nanjing, China; (approval number: 2019ZDSYLL021-P01). Waiver of informed consent was granted by the ethics committee due to the retrospective and anonymized nature of the study.

## Acknowledgment

We express our gratitude to Professor Pingsheng Chen from the Department of Pathology, School of Medicine, Southeast University, for providing access to laboratory facilities and offering technical guidance throughout this study. Additionally, we acknowledge Dr. Hui Xu from the Department of Immunology, School of Medicine, Southeast University, for generously providing the SKOV3 and SKOV3/DDP cell lines.

## Funding

This work was supported by the National Natural Science Foundation of China (81872122).

## Conflict of Interest

The authors declare no conflict of interest.

## Supplementary Material

Supplementary material associated with this article can be found, in the online version, at <https://doi.org/10.31083/CEOG39988>.

## Declaration of AI and AI-Assisted Technologies in the Writing Process

During the preparation of this work, the authors employed DeepSeek and ChatGPT to assist with language polishing and expression refinement. Following the use of these tools, the authors thoroughly reviewed and edited the content as necessary, and assumes full responsibility for the integrity and accuracy of the published material.

## References

- [1] Ostrowska-Lesko M, Rajtak A, Moreno-Bueno G, Bobinski M. Scientific and clinical relevance of non-cellular tumor microenvironment components in ovarian cancer chemotherapy resistance. *Biochimica et Biophysica Acta. Reviews on Cancer*. 2024; 1879: 189036. <https://doi.org/10.1016/j.bbcan.2023.189036>.
- [2] Yu M, Zhu Y, Teng L, Cui J, Su Y. Can Circulating Cell-Free DNA or Circulating Tumor DNA Be a Promising Marker in Ovarian Cancer? *Journal of Oncology*. 2021; 2021: 6627241. <https://doi.org/10.1155/2021/6627241>.
- [3] Saani I, Raj N, Sood R, Ansari S, Mandviwala HA, Sanchez E, *et al*. Clinical Challenges in the Management of Malignant Ovarian Germ Cell Tumours. *International Journal of Environmental Research and Public Health*. 2023; 20: 6089. <https://doi.org/10.3390/ijerph20126089>.
- [4] Li X, Wang Q, Ai L, Cheng K. Unraveling the activation process and core driver genes of HSCs during cirrhosis by single-cell transcriptome. *Experimental Biology and Medicine* (Maywood, N.J.). 2023; 248: 1414–1424. <https://doi.org/10.1177/15353702231191109>.
- [5] Gong D, Zhang Q, Chen LY, Yu XH, Wang G, Zou J, *et al*. Coiled-coil domain-containing 80 accelerates atherosclerosis development through decreasing lipoprotein lipase expression via ERK1/2 phosphorylation and TET2 expression. *European Journal of Pharmacology*. 2019; 843: 177–189. <https://doi.org/10.1016/j.ejphar.2018.11.009>.
- [6] Wang WD, Wu GY, Bai KH, Shu LL, Chi PD, He SY, *et al*. A prognostic stemness biomarker *CCDC80* reveals acquired drug resistance and immune infiltration in colorectal cancer. *Clinical and Translational Medicine*. 2020; 10: e225. <https://doi.org/10.1002/ctm2.225>.
- [7] Yu M, Peng J, Lu Y, Li S, Ding K. Silencing immune-infiltrating biomarker *CCDC80* inhibits malignant characterization and tumor formation in gastric cancer. *BMC Cancer*. 2024; 24: 724. <https://doi.org/10.1186/s12885-024-12451-y>.
- [8] Ferraro A, Schepis F, Leone V, Federico A, Borbone E, Pallante P, *et al*. Tumor suppressor role of the *CL2/DRO1/CCDC80* gene in thyroid carcinogenesis. *The Journal of Clinical Endocrinol-*



- ogy and Metabolism. 2013; 98: 2834–2843. <https://doi.org/10.1210/jc.2012-2926>.
- [9] Grill JI, Neumann J, Herbst A, Hiltwein F, Ofner A, Marschall MK, *et al.* DRO1 inactivation drives colorectal carcinogenesis in ApeMin/+ mice. *Molecular Cancer Research: MCR*. 2014; 12: 1655–1662. <https://doi.org/10.1158/1541-7786.MC.R-14-0205-T>.
- [10] Pan WW, Moroishi T, Koo JH, Guan KL. Cell type-dependent function of LATS1/2 in cancer cell growth. *Oncogene*. 2019; 38: 2595–2610. <https://doi.org/10.1038/s41388-018-0610-8>.
- [11] Paullin T, Powell C, Menzie C, Hill R, Cheng F, Martyniuk CJ, *et al.* Spheroid growth in ovarian cancer alters transcriptome responses for stress pathways and epigenetic responses. *PLoS One*. 2017; 12: e0182930. <https://doi.org/10.1371/journal.pone.0182930>.
- [12] Yuan H, Yu Q, Pang J, Chen Y, Sheng M, Tang W. The Value of the Stemness Index in Ovarian Cancer Prognosis. *Genes*. 2022; 13: 993. <https://doi.org/10.3390/genes13060993>.
- [13] Fan Y, Cheng H, Liu Y, Liu S, Lowe S, Li Y, *et al.* Metformin anticancer: Reverses tumor hypoxia induced by bevacizumab and reduces the expression of cancer stem cell markers CD44/CD117 in human ovarian cancer SKOV3 cells. *Frontiers in Pharmacology*. 2022; 13: 955984. <https://doi.org/10.3389/fphar.2022.955984>.
- [14] Terraneo N, Jacob F, Dubrovskaya A, Grünberg J. Novel Therapeutic Strategies for Ovarian Cancer Stem Cells. *Frontiers in Oncology*. 2020; 10: 319. <https://doi.org/10.3389/fonc.2020.00319>.
- [15] Wang Y, Zong X, Mitra S, Mitra AK, Matei D, Nephew KP. IL-6 mediates platinum-induced enrichment of ovarian cancer stem cells. *JCI Insight*. 2018; 3: e122360. <https://doi.org/10.1172/jci.insight.122360>.
- [16] Huang Y, Hong W, Wei X. The molecular mechanisms and therapeutic strategies of EMT in tumor progression and metastasis. *Journal of Hematology & Oncology*. 2022; 15: 129. <https://doi.org/10.1186/s13045-022-01347-8>.
- [17] Pan G, Liu Y, Shang L, Zhou F, Yang S. EMT-associated microRNAs and their roles in cancer stemness and drug resistance. *Cancer Communications (London, England)*. 2021; 41: 199–217. <https://doi.org/10.1002/cac2.12138>.
- [18] Ang HL, Mohan CD, Shanmugam MK, Leong HC, Makvandi P, Rangappa KS, *et al.* Mechanism of epithelial-mesenchymal transition in cancer and its regulation by natural compounds. *Medicinal Research Reviews*. 2023; 43: 1141–1200. <https://doi.org/10.1002/med.21948>.
- [19] Kielbik M, Przygodzka P, Szulc-Kielbik I, Klink M. Snail transcription factors as key regulators of chemoresistance, stemness and metastasis of ovarian cancer cells. *Biochimica et Biophysica Acta. Reviews on Cancer*. 2023; 1878: 189003. <https://doi.org/10.1016/j.bbcan.2023.189003>.
- [20] Xue W, Yang L, Chen C, Ashrafizadeh M, Tian Y, Sun R. Wnt/ $\beta$ -catenin-driven EMT regulation in human cancers. *Cellular and Molecular Life Sciences: CMLS*. 2024; 81: 79. <https://doi.org/10.1007/s00018-023-05099-7>.
- [21] Wang W, Liu W, Chen Q, Yuan Y, Wang P. Targeting CSC-related transcription factors by E3 ubiquitin ligases for cancer therapy. *Seminars in Cancer Biology*. 2022; 87: 84–97. <https://doi.org/10.1016/j.semcancer.2022.11.002>.
- [22] Chen B, Liu J. Advances in ovarian tumor stem cells and therapy. *Cell Biochemistry and Biophysics*. 2024; 82: 1871–1892. <https://doi.org/10.1007/s12013-024-01385-8>.
- [23] Pieterse Z, Amaya-Padilla MA, Singomat T, Binju M, Madjid BD, Yu Y, *et al.* Ovarian cancer stem cells and their role in drug resistance. *The International Journal of Biochemistry & Cell Biology*. 2019; 106: 117–126. <https://doi.org/10.1016/j.biocel.2018.11.012>.
- [24] Raza S, Rajak S, Tewari A, Gupta P, Chattopadhyay N, Sinha RA, *et al.* Multifaceted role of chemokines in solid tumors: From biology to therapy. *Seminars in Cancer Biology*. 2022; 86: 1105–1121. <https://doi.org/10.1016/j.semcancer.2021.12.011>.
- [25] Rinne N, Christie EL, Ardasheva A, Kwok CH, Demchenko N, Low C, *et al.* Targeting the PI3K/AKT/mTOR pathway in epithelial ovarian cancer, therapeutic treatment options for platinum-resistant ovarian cancer. *Cancer Drug Resistance (Alhambra, Calif.)*. 2021; 4: 573–595. <https://doi.org/10.20517/cdr.2021.05>.
- [26] Zheng P, Fan M, Liu H, Zhang Y, Dai X, Li H, *et al.* Self-Propelled and Near-Infrared-Phototoxic Photosynthetic Bacteria as Photothermal Agents for Hypoxia-Targeted Cancer Therapy. *ACS Nano*. 2021; 15: 1100–1110. <https://doi.org/10.1021/acsnano.0c08068>.
- [27] Lu Q, Yang D, Li H, Niu T, Tong A. Multiple myeloma: signaling pathways and targeted therapy. *Molecular Biomedicine*. 2024; 5: 25. <https://doi.org/10.1186/s43556-024-00188-w>.
- [28] He Y, Sun MM, Zhang GG, Yang J, Chen KS, Xu WW, *et al.* Targeting PI3K/Akt signal transduction for cancer therapy. *Signal Transduction and Targeted Therapy*. 2021; 6: 425. <https://doi.org/10.1038/s41392-021-00828-5>.
- [29] Zhao H, Wu L, Yan G, Chen Y, Zhou M, Wu Y, *et al.* Inflammation and tumor progression: signaling pathways and targeted intervention. *Signal Transduction and Targeted Therapy*. 2021; 6: 263. <https://doi.org/10.1038/s41392-021-00658-5>.
- [30] Wang W, Shi B, Cong R, Hao M, Peng Y, Yang H, *et al.* RING-finger E3 ligases regulatory network in PI3K/AKT-mediated glucose metabolism. *Cell Death Discovery*. 2022; 8: 372. <https://doi.org/10.1038/s41420-022-01162-7>.
- [31] Janku F. Phosphoinositide 3-kinase (PI3K) pathway inhibitors in solid tumors: from laboratory to patients. *Cancer Treatment Reviews*. 2017; 59: 93–101. <https://doi.org/10.1016/j.ctrv.2017.07.005>.
- [32] Liu J, Yang J, Hou Y, Zhu Z, He J, Zhao H, *et al.* Casticin inhibits nasopharyngeal carcinoma growth by targeting phosphoinositide 3-kinase. *Cancer Cell International*. 2019; 19: 348. <https://doi.org/10.1186/s12935-019-1069-6>.
- [33] Matassa DS, Amoroso MR, Lu H, Avolio R, Arzeni D, Procaccini C, *et al.* Oxidative metabolism drives inflammation-induced platinum resistance in human ovarian cancer. *Cell Death and Differentiation*. 2016; 23: 1542–1554. <https://doi.org/10.1038/cdd.2016.39>.
- [34] Boussios S, Karathanasi A, Cooke D, Neille C, Sadauskaitė A, Moschetta M, *et al.* PARP Inhibitors in Ovarian Cancer: The Route to “Ithaca”. *Diagnostics (Basel, Switzerland)*. 2019; 9: 55. <https://doi.org/10.3390/diagnostics9020055>.
- [35] Ghose A, Gullapalli SVN, Chohan N, Bolina A, Moschetta M, Rassy E, *et al.* Applications of Proteomics in Ovarian Cancer: Dawn of a New Era. *Proteomes*. 2022; 10: 16. <https://doi.org/10.3390/proteomes10020016>.
- [36] Huang C, Zhou Y, Feng X, Wang J, Li Y, Yao X. Delivery of Engineered Primary Tumor-Derived Exosomes Effectively Suppressed the Colorectal Cancer Chemoresistance and Liver Metastasis. *ACS Nano*. 2023; 17: 10313–10326. <https://doi.org/10.1021/acsnano.3c00668>.
- [37] Li X, Du Y. Lactate Metabolism Subtypes Analysis Reveals CCDC80 as a Novel Prognostic Biomarker in Gastric Cancer. *Journal of Cancer*. 2024; 15: 5557–5576. <https://doi.org/10.7150/jca.97640>.
- [38] Ghose A, McCann L, Makker S, Mukherjee U, Gullapalli SVN, Erekkath J, *et al.* Diagnostic biomarkers in ovarian cancer: advances beyond CA125 and HE4. *Therapeutic Advances in Medical Oncology*. 2024; 16: 17588359241233225. <https://doi.org/10.1177/17588359241233225>.